International Journal of GEOMATE, May, 2016, Vol. 10, Issue 21, pp. 1950-1955
Geotec., Const. Mat. & Env., ISSN: 2186-2982(Print), 2186-2990(Online), Japan

NUMERICAL EXPERIMENT FOR VIRTUAL PLASTER MODEL TESTS SIMULATING BLOCK SHEAR TESTS

Tatsuro Nishiyama[1] and Takashi Hasegawa[2]

[1]Faculty of Agriculture, Ehime University, Japan; [2]Professor Emeritus, Kyoto University, Japan

ABSTRACT: The strength of in-situ rock masses has been estimated by in-situ rock shear tests for a long time. However, the mechanisms for the appearance of strength in such tests have not been clarified sufficiently. This paper presents the results of a numerical analysis of virtual plaster model tests used to simulate block shear tests, which are of a kind of in-situ test. In the authors' former study, results were obtained for rock shear tests, another kind of in-situ test, along with real plaster model tests and finite element analyses. In the present study, some cases simulating block shear tests were analyzed. The appearance and propagation of cracks in the testing process were simulated with enhanced elements, which represented the displacement discontinuity in each element, as in the former analysis. The results were compared with the former results to investigate the differences between the two conditions. The shear strength in the two sets of results was found to be generally similar; however, there were some small differences. The patterns for the appearance and propagation of cracks differed from each other, while some common features also appeared. The concentration of stress in the two testing processes occurred in different parts of the materials under the two conditions, and this led to differences in both the failure mechanism and the shear strength.

Keywords: Block Shear Test, Rock Mass, Shear Strength, Crack, Finite Element Analysis

1. INTRODUCTION

The strength of in-situ rock masses, such as the rock foundations of large dams, has been estimated by in-situ rock shear tests for a long time. The method for such tests is constructed as a direct shear test, and the results have been treated as the shear strength with Coulomb's criteria in many practical applications. However, the mechanisms for the appearance of strength in such tests have not been clarified sufficiently.

Two kinds of methods for such tests have recently been prescribed by, for example, the Japanese Geotechnical Society [1]. One is the rock shear test, where the rock to be tested is shaped in a block form and loads are applied to the rock block. The other is the block shear test, where a concrete block is set on the rock to be tested and loads are applied to the concrete block.

The authors [2]-[3] have investigated some basic features of the rock shear test with some plaster model tests and a numerical analysis. Although the shear strength and the displacement obtained from the numerical analysis were lower than those obtained from the real plaster model tests, the mechanical features, including the failure mechanisms, generally resembled those of the real plaster model tests.

The block shear test, which is another kind of in-situ test, is different from the rock shear test in terms of the stiffness of the block to be loaded. This paper presents the results of a numerical analysis of virtual plaster model tests used to simulate the block shear test. Virtual plaster model tests were adopted because it would be tough to conduct real plaster model tests which resemble the authors' former ones for simulating block shear tests due to the difficulty in the bonding between the other materials. The results were compared with the former results to investigate the differences between the two kinds of in-situ tests.

2. METHODS

2.1 Object of Analysis

The loading methods used in the in-situ tests are schematically shown in Fig. 1. In this figure, (a) and (b) represent the sections of the blocks to be loaded. In each testing process, firstly, the normal force, F_N, is given and kept constant, and secondly, the inclined force, F_I, is increasingly applied. Such loading causes direct shear on the anticipated shear plane.

Figure 2(a) shows the shape of the plaster models which were used in the authors' former study. The conditions were set to be similar to those in the rock shear test, except that both surfaces were confined with clear plates to create the plane strain condition. Figure 2(b) presents the virtual model for simulating the block shear test, resembling the plaster model in Fig. 2(a), except that the block part is almost rigid.
In order to compare only the rigidity of the blocks, the steel cap was kept separated from the block part even in the block shear test type (Fig. 2(b)), as was done in the rock shear test type (Fig. 2(a)).

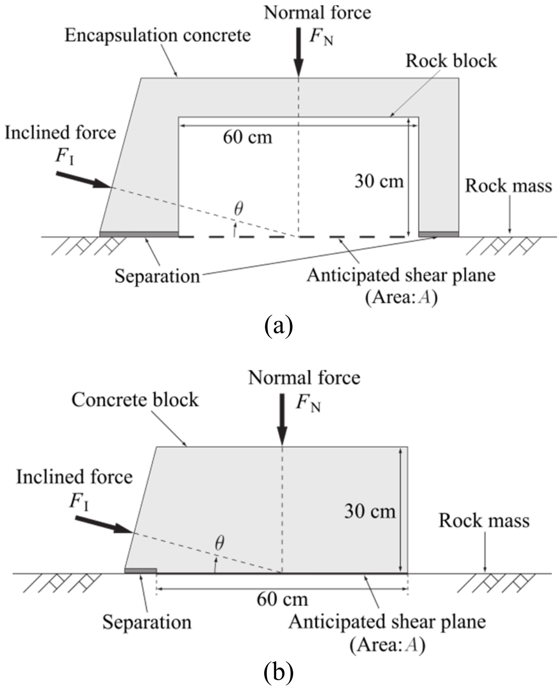

In both tests, normal stress σ and shear stress τ are given as
$\sigma = (F_N + F_I \sin\theta) / A$, $\tau = F_I \cos\theta / A$
on the anticipated shear plane. The maximum value for τ and the corresponding value for σ are used to determine the strength. Initial normal stress σ_n is given as
$\sigma_n = F_N / A$.

Fig. 1 Two types of in-situ rock shear tests: (a) Rock shear test, (b) Block shear test.

The former plaster model tests were conducted for dozens of cases under different values for the initial normal stress, σ_n , on both intact and layered models, and all the cases were numerically analyzed (Nishiyama and Hasegawa [3]). In the new analysis, shown in this paper, tests were conducted on the intact model considering 7 different levels of initial stress, namely, σ_n = 0.375, 0.625, 1.25, 2.5, 3.75, 5, 7.5 (MPa).

2.2 Given Conditions and Procedure

The numerical model for the virtual model in Fig. 2(b) was composed of finite elements, as shown in Fig. 3. All the elements were simple constant strain triangles. The material parameters are given in Table 1; they are the same as those in the authors' former analysis.

At the boundary between the cap and the block, double nodes were adopted for the contact analysis. A simple contact analysis was also conducted on the outer boundary; however, the boundary between the

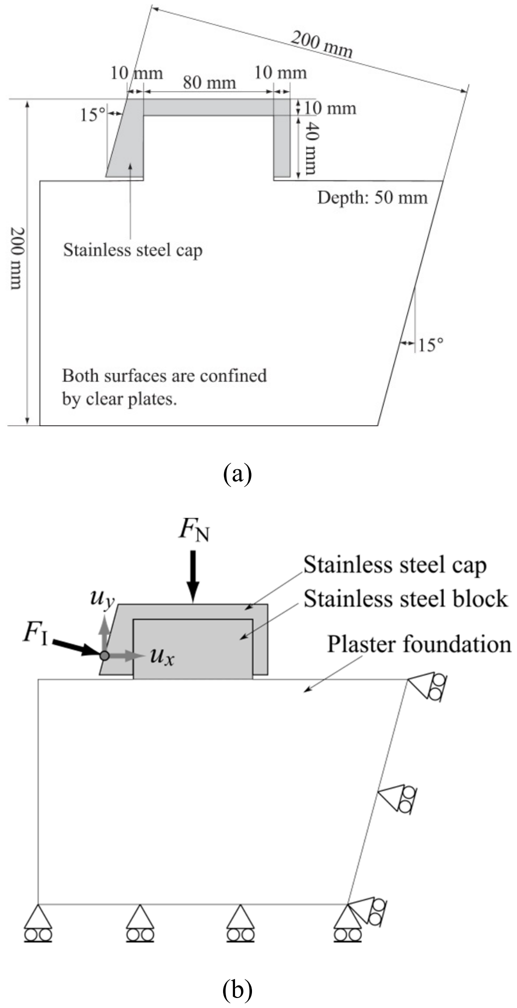

Fig. 2 Plaster models: (a) Model for simulating rock shear tests (Nishiyama and Hasegawa [2]), (b) Virtual model for simulating block shear tests.

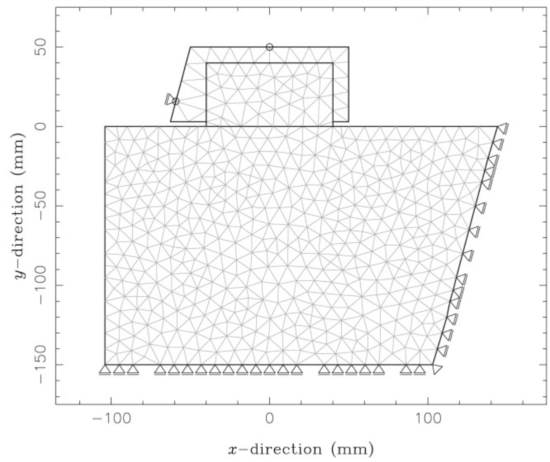

Fig. 3 Numerical model for simulating the virtual plaster model for simulating block shear tests, which are shown in Fig. 2(b).

Table 1 Material properties.

Material	Item	Value
Plaster	Density (kg/m^3) *	1,121
	Elastic modulus (MPa)	3,697
	Poisson's ratio	0.35
	Uniaxial compressive strength, σ_{ci} (MPa)	16.56
	Uniaxial tensile strength (MPa)	−2.844
	Hoek-Brown's constant, m	5.65
	Hoek-Brown's constant, s	1
Steel	Elastic modulus (GPa)	200
	Poisson's ratio	0.3

* Density was ignored in the analysis.

The strength of the plaster material was described as Hoek-Brown's failure criteria (Hoek [4]), namely,

$$\sigma_1 = \sigma_3 + \sqrt{m\,\sigma_{ci}\sigma_3 + s\,\sigma_{ci}^{\ 2}}$$

where σ_1 and σ_3 are the major and the minor principal stress values, respectively.

block and the foundation was treated as an ordinary element boundary with single nodes because the block and the foundation should be bonded through the loading process.

An incremental analysis was conducted in the same way as in the former analysis, as follows. In every case, the boundary condition corresponding to the normal load, F_N, was given as the nodal force in the first step. Then, from the second step, the boundary condition corresponding to the inclined load, F_I, was given incrementally as the nodal displacement.

To simulate crack propagation, the CST elements whose stress had reached the material strength were replaced at every step with enhanced elements, each of which included an interface within itself (Bolzon [5]).

When the stress of the enhanced elements reached the material strength, the elastic modulus of the concerned elements was reduced to 10% of the original value to express the crushed material.

Failure was basically not considered for the steel elements. However, only the steel elements which were adjacent to the plaster elements where failure occurred were replaced with enhanced elements on account of the activation on the interface nodes of the enhanced plaster elements.

3. RESULTS

Figure 4 shows the macroscopic shear strength values which were obtained from the analysis. In this figure, the values for each type differ from one another. The shear strength for the block shear test type is smaller than that for the rock shear test type in the lower normal stress range, and such a tendency seems to make the row of data points become straighter. In the higher normal stress range, the results of the two types of tests are not the same; however, they commonly appear to be lower than the material strength.

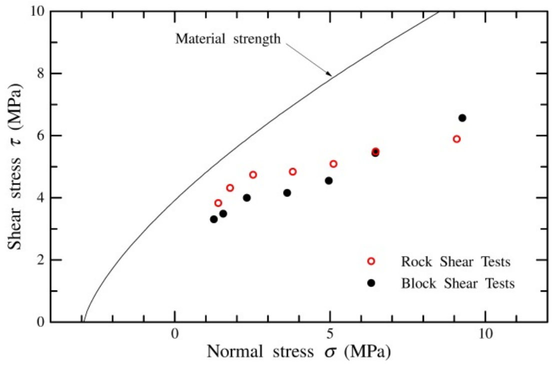

Fig. 4 Comparison of shear resistance values between the two types of tests.

Figure 6 shows the cracking sequence in one of the cases of the block shear test type. Referring to Fig. 5, the first small failure which localized on the side opposite to the loading side of the inclined force corresponds to the peak shear stress. Then, in Fig. 5, block heaving has already appeared. After that, small failures occurred gradually along the base of the block, and finally, the block was completely separated from the foundation. Referring to the former results for the rock shear test type, shown in Fig. 7, the width of the broken zone is narrower in the block shear test type.

The difference in the features of the cracking sequences, according to the initial normal stress, is much less noticeable than the difference in the rock shear test type. The curved propagation of a tensile crack just under the loading side happened only in the cases of the lower normal stress with the rock shear test type, whereas it occurred only in the cases of the higher normal stress with the block shear test type. Figure 8 shows the crack distribution at the residual state in one of the cases under higher normal stress.

4. DISCUSSION

The block is stiffer than the foundation to be broken in the block shear test type, while the stiffness is the same in the rock shear test type. Therefore, the stress distribution in the foundation under the block would need to be made to be nearly uniform in the block shear test type. On the other hand, the non-uniform stress distribution seemed to cause a reduction in strength in the model tests of

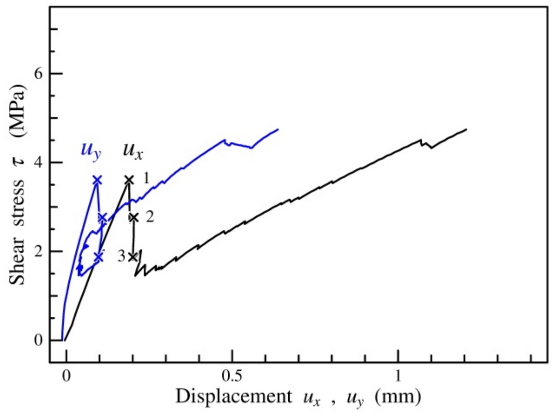

Fig. 5 Relation between the displacement and the shear stress in the case of $\sigma_n = 0.625$ MPa. The numbers correspond to those in Fig. 6.

the rock shear test type because the peak shear stress appeared with a small fatal failure in every case. Before the analysis, therefore, the strength in the block shear test type was expected to be higher than that in the rock shear test type.

In the analysis of the block shear test type, uniform stress distributions certainly appeared, as shown in Fig. 9(b). However, the stress concentration caused on the side opposite to the loading side was remarkable. The reason is that it is easier to transmit the compressional stress to the opposite side with a stiffer block. Such a stress concentration caused a decrease in strength in the analysis. This reduction in strength corresponds to the knowledge reported by the Japanese Geotechnical Society [6]. In the rock shear test type, the regularity of the row of data points for the shear strength varied through the normal stress ranges according to the variation in failure mechanisms. The variation in failure mechanisms, according to the normal stress, was very little in the block shear test type; however, the obvious propagation of a tensile crack under the loading side appeared only in each case under the higher normal stress. Once again, referring to the details in Fig. 4, the row of data points appears to be divided into two straight rows which consist of three points each, and the data point in the center seems to represent the transitional state. Such a variation in failure mechanisms, including the variation in the directions of the cracks, should also be related to that in the rock shear test type.

5. CONCLUSION

A finite element analysis was carried out for virtual plaster model tests to investigate the basic mechanisms of block shear tests. From the analysis, some differences between block shear tests and rock shear tests were found.

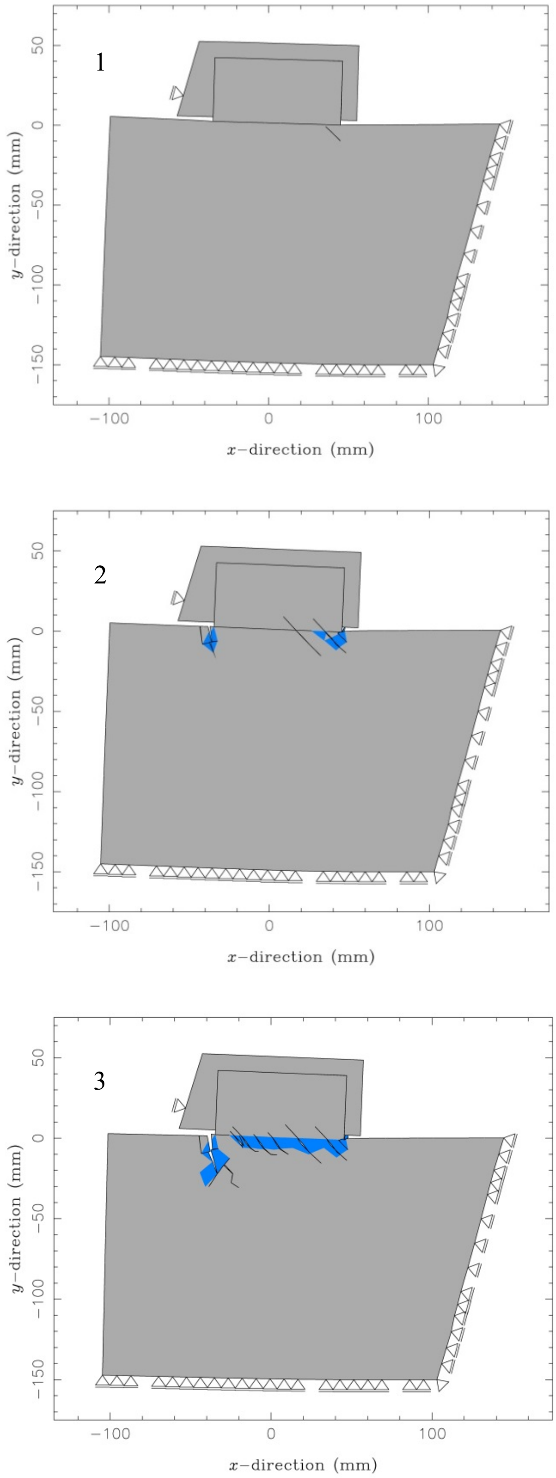

Fig. 6 Cracking sequence in the case of lower normal stress level, $\sigma_n = 0.625$ MPa, of the block shear test type. Displacement is emphasized as 30 times. The blue areas represent the regions where the elastic modulus has been reduced. The numbers correspond to those in Fig. 5.

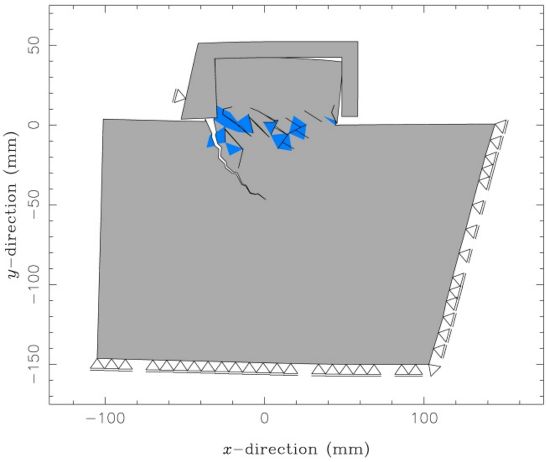

Fig. 7 Crack distribution at the residual state in the case of σ_n = 0.625 MPa of the rock shear test type (Nishiyama and Hasegawa [3]).

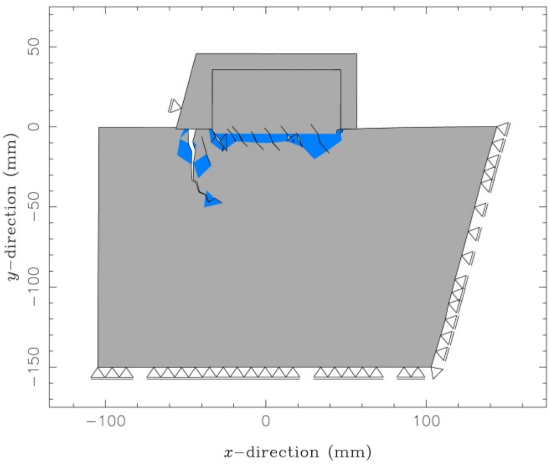

Fig. 8 Crack distribution at the residual state in the case of higher normal stress level, σ_n = 3.75 MPa, of the block shear test type.

The difference between block shear tests and rock shear tests is the degree of stiffness of the blocks. This in turn causes a difference in the distribution of stress in the rock to be broken and brings about changes in the failure mechanisms. Such a difference also leads to a difference in the macroscopic shear strength.

The macroscopic shear strength is lower in the block shear tests than in the rock shear tests under lower normal stress. Such a tendency makes the row of data points become straighter.

The above conclusions are of course only certain for the conditions given in limited cases. Further investigations in the future, for example, a detailed stress analysis or additional analyses for many different cases, are required to obtain more general conclusions.

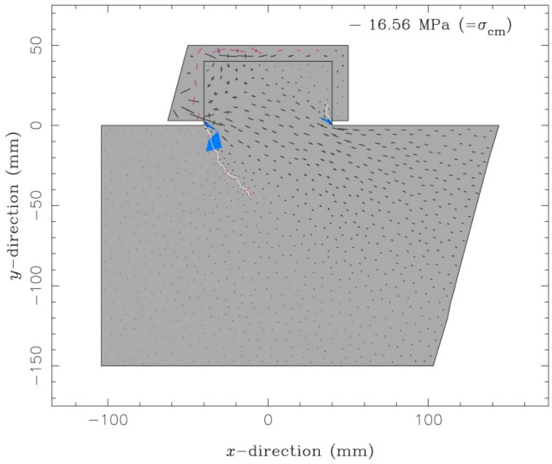

(a)

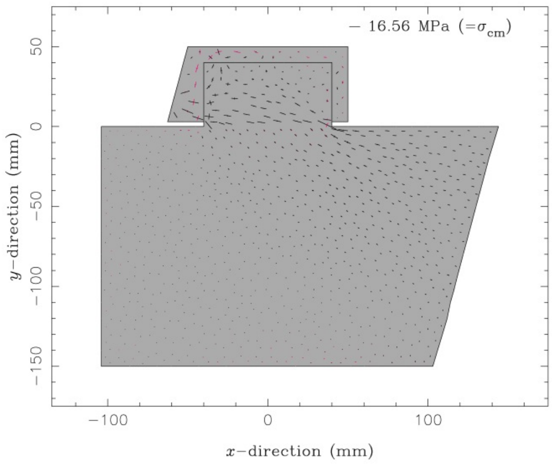

(b)

Fig. 9 Comparison of the stress distributions at the peaks of the shear stress in the cases of σ_n = 0.625 MPa: (a) Rock shear test type, (b) Block shear test type. The segments represent the principal stress axes, shown in black for compression and in magenta for tension, and $\sigma_{cm}=\sqrt{s\sigma_{ci}^2}$ represents the com-pressional strength of mass of the material. In the foundation part, just under each block, the compressional stress is distrib-uted widely in (a), while there is little load in (b).

6. ACKNOWLEDGEMENTS

This work was supported by JSPS KAKENHI Grant Number 25450362.

7. REFERENCES

[1] The Japanese Geotechnical Society, "Method for In-situ Direct Shear Test on Rocks", JGS 3511-2004, 2004.
[2] Nishiyama T, Hasegawa T, "A fundamental study on the strength measured by in-situ rock shear tests", in Proc. 3rd Int. Symp. on Deformation Characteristics of Geomaterials, 2003, pp. 97-104.
[3] Nishiyama T, Hasegawa T, "A practical use of the finite element with an embedded interface for simulating the direct shear on brittle materials", in Proc. 14th IACMAG, 2014, pp. 323-327.
[4] Hoek E, "Strength of Jointed Rock Masses", Géotechnique, Vol. 3, 1983, pp. 185-223.
[5] Bolzon G, "Formulation of a triangular finite element with an embedded interface via isoparametric mapping", Computational Mechanics, Vol. 27, 2001, pp. 463-473.
[6] The Japanese Geotechnical Society, Methods of Determination of Geotechnical Constants for Design –Rock Mass Edition-. Tokyo: The Japanese Geotechnical Society, 2007, p. 12 (in Japanese).

International Journal of GEOMATE, May, 2016, Vol. 10, Issue 21, pp. 1950-1955.
MS No. 5300 received on June 15, 2015 and reviewed under GEOMATE publication policies.

Corresponding Author: Tatsuro Nishiyama